

Direct observation of imprinted antiferromagnetic vortex states in CoO/Fe/Ag(001) discs

J. Wu¹, D. Carlton², J. S. Park¹, Y. Meng^{1,3}, E. Arenholz⁴, A. Doran⁴, A. T. Young⁴, A. Scholl⁴, C. Hwang⁵, H. W. Zhao³, J. Bokor² and Z. Q. Qiu^{1*}

In magnetic thin films, a magnetic vortex is a state in which the magnetization vector curls around the centre of a confined structure¹. In a thin-film disc, vortex states are characterized by the vortex polarity and the winding number^{2,3}. In ferromagnetic (FM) discs, these two parameters have been shown to govern many fundamental properties of the vortex, such as its gyroscopic rotation⁴, polarity reversal⁵⁻⁷, core motion⁸ and vortex-pair excitation⁹. In antiferromagnetic (AFM) discs¹⁰, in contrast, there has been only indirect evidence for a vortex state, obtained through the observation of induced FM-ordered spins in the AFM disc¹¹⁻¹⁴. Here we report the direct observation of an AFM vortex state in the AFM layer of an AFM/FM bilayer system. We have fabricated single-crystalline NiO/Fe/Ag(001) and CoO/Fe/Ag(001) discs, and using X-ray magnetic linear dichroism techniques we observe two types of AFM vortex, one of which has no analogue in FM structures. We also show that a frozen AFM vortex can bias an FM vortex at low temperature.

Single-crystalline NiO/Fe(12 nm)/Ag(001) and CoO/Fe(12 nm)/Ag(001) films were grown by molecular beam epitaxy and patterned into discs using a focused ion beam. The FM Fe and AFM NiO and CoO were measured at the Advanced Light Source of Lawrence Berkeley National Laboratory by X-ray magnetic circular dichroism (XMCD) and X-ray magnetic linear dichroism (XMLD). Although the XMCD measurement is a standard method, the XMLD measurement on NiO and CoO in our experiment was made at the Ni L2 edge and Co L3 edge by changing the X-ray linear polarization angle (ϕ) relative to the Fe [001] magnetization axis, which is parallel to the NiO or CoO [110] crystalline axis (Fig. 1a; ref. 15). Figure 1 represents a typical CoO XMLD result from CoO (3 nm)/Fe (12 nm)/Ag(001) with the XMLD signal defined by the so-called L3 ratio (R_{L3}), which is the X-ray absorption intensity at the photon energy $E = 778.1$ eV divided by the absorption intensity at $E = 778.9$ eV (ref. 15). The L3 ratio follows the expected $\cos^2\phi$ dependence for all CoO thicknesses. As the L3 ratio under this condition should reach its maximum value for X-ray polarization parallel to the CoO spin axis¹⁶⁻¹⁸, the R_{L3} result in Fig. 1b shows that the CoO spins are coupled collinearly to the Fe spins at smaller CoO thickness ($d_{\text{CoO}} = 0.6$ nm) and perpendicularly to the Fe spins at larger CoO thickness ($d_{\text{CoO}} = 3.0$ nm). This collinear to 90° coupling transition was also reported in the NiO/Fe(001) system as a function of NiO thickness¹⁹. The underlying mechanism of this coupling transition remains unclear so far and has been a focus of research in this field.

Element-specific magnetic domains were imaged for both the FM Fe and the AFM NiO (CoO) of the bilayer discs at

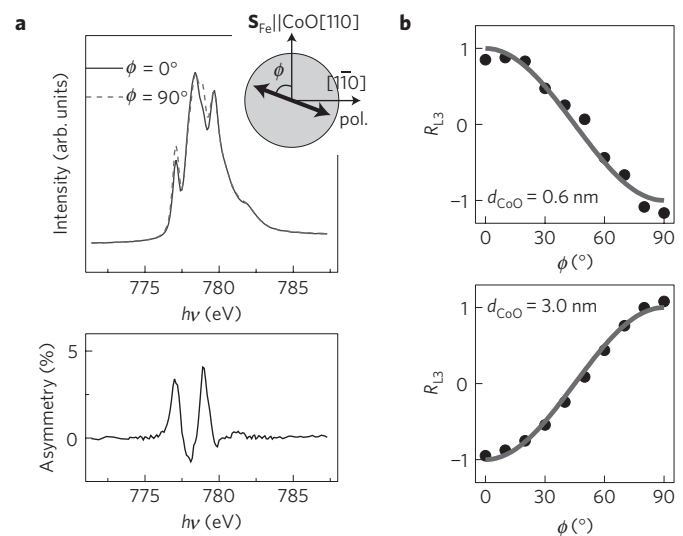


Figure 1 | XMLD spectra of CoO from CoO/Fe/Ag(001). **a**, The X-ray absorption spectra with the X-ray polarization parallel ($\phi = 0^\circ$) and perpendicular ($\phi = 90^\circ$) to the Fe magnetization direction. The difference between these two absorption spectra shows the XMLD effect. **b**, The opposite dependence of the L3 ratio (R_{L3}) of the XMLD on the polarization angle shows that the CoO spins are coupled collinearly (at $d_{\text{CoO}} = 0.6$ nm) and perpendicularly (at $d_{\text{CoO}} = 3.0$ nm) to the Fe spins, respectively.

low temperature using photoemission electron-beam microscopy (PEEM). Although the FM Fe discs exhibit the expected FM vortices for both circular and square discs, the AFM domain imaging of the NiO and CoO discs reveals unambiguously the existence of the AFM vortex state in the NiO and CoO discs (Fig. 2). It should be emphasized that, in addition to the majority AFM-ordered spins (compensated spins), the AFM layer in an AFM/FM bilayer system sometimes could contain a small number of FM-ordered spins (uncompensated spins) induced by the FM layer. Although the induced FM-ordered spins are located at the AFM/FM interface and have properties that resemble those of the FM layer, the majority AFM-ordered spins represent the magnetic properties of the AFM layer. The AFM vortex state reported in previous works¹¹⁻¹³ was actually from the FM-ordered uncompensated spins in the AFM layer at the AFM/FM interface rather than from the majority AFM-ordered compensated spins in the AFM layer. As the XMLD signal in our work is from the AFM-ordered compensated spins, the NiO and

¹Department of Physics, University of California at Berkeley, Berkeley, California 94720, USA, ²Department of Electrical Engineering and Computer Sciences, University of California at Berkeley, Berkeley, California 94720, USA, ³Institute of Physics, Chinese Academy of Science, Beijing 100190, China, ⁴Advanced Light Source, Lawrence Berkeley National Laboratory, Berkeley, California 94720, USA, ⁵Korea Research Institute of Standards and Science, Yuseong, Daejeon 305-340, Korea. *e-mail: qiu@socrates.berkeley.edu.

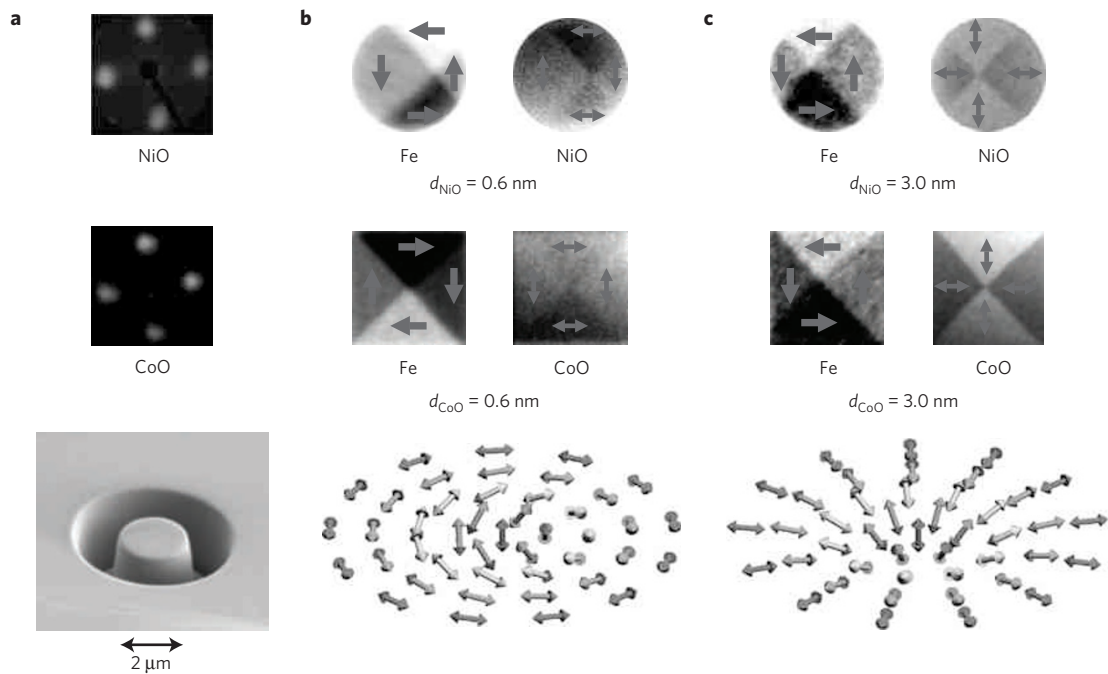


Figure 2 | Element-specific magnetic-domain images of NiO/Fe and CoO/Fe discs. **a**, Low-energy electron diffraction patterns and scanning electron microscope image of the single-crystalline NiO/Fe/Ag(001) and CoO/Fe/Ag(001) discs. **b,c**, The NiO and CoO discs exhibit curling vortices at 0.6 nm and CoO thickness (**b**) and divergent vortices at 3.0 nm NiO and CoO thickness (**c**). The diameter of the discs is 2 μm , the same as the length of the square patterns. The divergent vortex is forbidden in an FM disc.

CoO vortices shown in Fig. 2 represent the first direct observation of the AFM vortex state from the AFM-ordered compensated spins, as opposed to the vortex state from the induced FM-ordered uncompensated spins. The AFM NiO and CoO vortices follow the same pattern as the Fe vortices, showing that the AFM vortex state is imprinted from the FM vortex through the AFM/FM interfacial interaction^{11–13}. We found that there exist two types of AFM vortex. In thinner NiO (CoO) films, the AFM spins are coupled collinearly with the Fe spins, so the AFM vortex has the conventional structure with the spins curling around the centre of the disc in the same manner as the FM vortex (Fig. 2b). However, in thicker NiO (CoO) films, the AFM spins are coupled perpendicularly to the Fe spins to result in an AFM vortex structure with a divergent spin configuration (Fig. 2c). The divergent vortex is forbidden both for an FM disc and for the FM-ordered uncompensated spins in an AFM disc because a divergent FM vortex would produce magnetic charges at the disc boundary to increase the magnetostatic energy. We believe that the divergent vortex is allowed only for the AFM-ordered compensated spins in an AFM disc because the opposite magnetic charges from the two magnetic sublattices of the AFM material cancel each other at the disc boundary.

PEEM measurements are not normally compatible with externally applied fields owing to interactions with the photoemitted electrons. However, when the isolation of the bilayer discs from the surrounding Fe thin film is not complete, the discs experience a local magnetic field produced by the surrounding Fe film. This field is mainly localized within the film and thus has limited effect on the photoemitted electrons outside the sample. Therefore, we can apply the PEEM technique to study the vortex state within the magnetic field of the surrounding Fe film. The strength of the magnetic field from the surrounding Fe film can be estimated as $H = -\int_0^{2\pi} (\cos\theta\sigma(\theta)d_{\text{Fe}}r d\theta)/r^2$, where d_{Fe} is the Fe film thickness, r is the radius of the cavity, θ is the azimuth angle and $\sigma(\theta)$ is the local magnetic surface charge density. When the surrounding Fe film has a uniform magnetization (Fig. 3a), the magnetic surface charge density is given by $\sigma(\theta) = -M_{\text{Fe}}\cos\theta$ so the magnetic field strength can

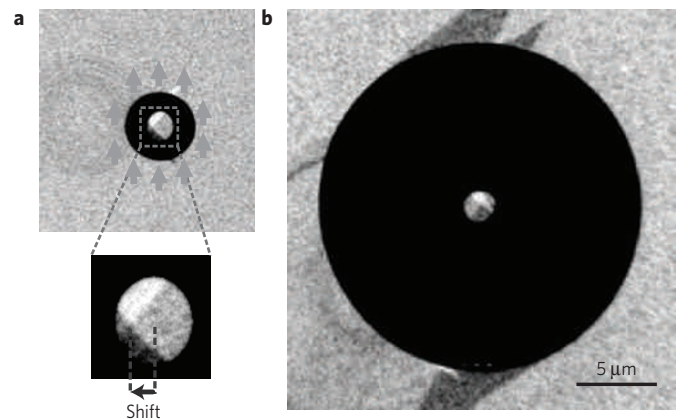


Figure 3 | Fe magnetic-domain images taken at room temperature on 2- μm -diameter CoO/Fe/Ag(001) discs. **a**, When the diameter of the outer circle is 4 μm , the magnetic field from the surrounding Fe film ($H \sim 32$ Oe) shifts the vortex core by ~ 0.5 μm . (The black ring corresponds to the region where the CoO/Fe film is completely removed.) **b**, When the diameter of the outer circle is 20 μm , the magnetic field from the surrounding Fe film is too weak to shift the vortex core.

be easily estimated as $H = (M_{\text{Fe}}d_{\text{Fe}})/r \int_0^{2\pi} \cos^2\theta d\theta = (\pi M_{\text{Fe}}d_{\text{Fe}})/r$. For $M_{\text{Fe}} = 1,700$ e.m.u. cm^{-3} , $d_{\text{Fe}} = 12$ nm and $r = 2$ μm (Fig. 3a), this estimation gives $H \approx 32$ Oe. The vortex-core position should shift in the transverse direction relative to the magnetic-field direction²⁰. Figure 3 shows the Fe PEEM images of the CoO (3 nm)/Fe (12 nm) disc at room temperature, which is above the Néel temperature of the CoO ($T_{\text{N}} = 291$ K). Under this condition, the CoO layer is in a paramagnetic state, so it will not bias the Fe disc magnetization in response to the external magnetic field. As expected, the vortex core of the Fe disc is shifted off-centre (Fig. 3a) by ~ 0.5 μm , which is about half of the disc radius ($R = 1$ μm). This amount of shift agrees with the experimental observation for a

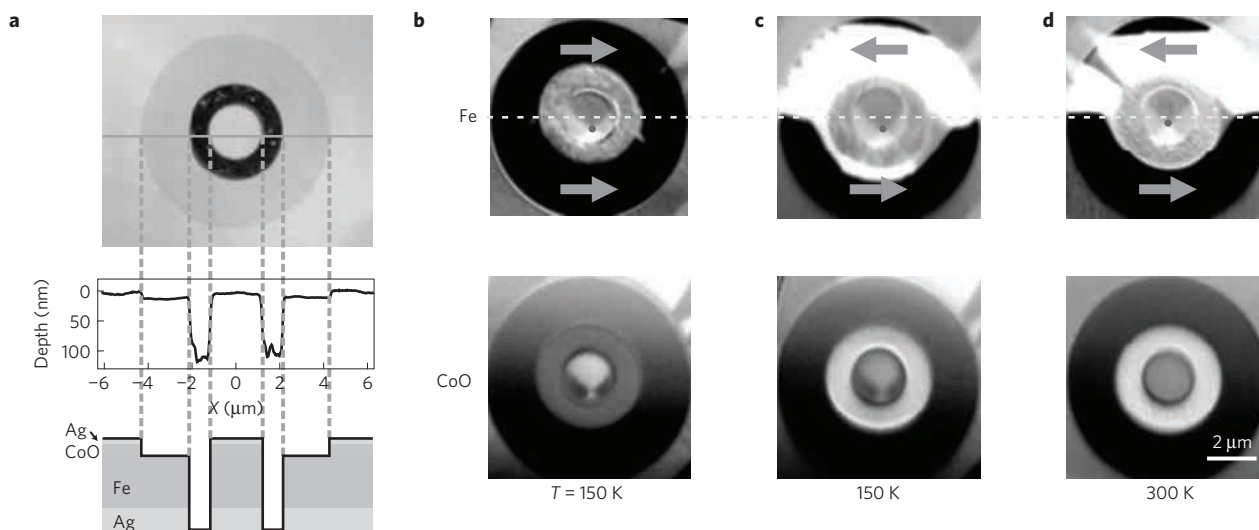


Figure 4 | Magnetic-domain images of a 2- μm -diameter CoO(3 nm)/Fe(12 nm)/Ag(001) disc under different conditions. **a, Atomic force microscope image, line profile and schematic drawing of the patterned CoO/Fe/Ag(001) sample. **b**, The local magnetic field produced by the Fe film surrounding the disc ($H \sim 32$ Oe) shifts the vortex-core position from the disc centre. **c**, After applying a 50-Oe magnetic-field pulse, the Fe surrounding film changed from a single-domain state to a multidomain state, so the local magnetic field produced by the Fe film surrounding the disc changed from $H \sim 32$ Oe to $H \sim 0$ Oe. The Fe vortex core remains in its off-centred position, showing the exchange-bias effect from the CoO vortex. **d**, After warming the sample to 300 K (above the CoO Néel temperature), the exchange-bias effect vanishes so the Fe vortex core moves to the centre position of the disc.**

vortex state within a ~ 30 Oe magnetic field²¹. The magnetic field produced by the surrounding Fe film is reduced by increasing the size of the ring that isolates the disc from the rest of the Fe film. When this field is reduced, the distance by which the vortex core shifts relative to the centre of the disc is reduced as expected (Fig. 3b).

The CoO/Fe disc was then cooled to 150 K to establish the CoO AFM order. Because this cooling took place in the presence of the local magnetic field provided by the surrounding Fe film, the AFM CoO layer is expected to produce an exchange bias^{22,23} on the FM Fe layer. If the magnetic field from the Fe magnetization outside the disc could be removed, the exchange bias should have the effect of retaining the Fe vortex in its current off-centre state¹². As we cannot apply an external magnetic field during the PEEM operation, we can only change the magnetic field to the CoO/Fe disc by changing the domain state of the surrounding Fe film to alter the magnetic surface-charge distribution at the boundary of the cavity. To change the surrounding Fe-film magnetic domains, we sputtered away the CoO overlayer of the surrounding Fe film using focused ion-beam sputtering with a careful control of the sputtering time (Fig. 4a). Note that a CoO (3 nm)/Fe (2.2 nm) film produces an exchange-bias field of 480 Oe in the CoO/Fe bilayer with a coercivity of 2,000–3,000 Oe (ref. 15). The Fe film without the CoO overlayer has a coercivity of only ~ 50 Oe. Thus we can apply a 50 Oe magnetic-field pulse to change the Fe surrounding-film domain state without affecting the CoO/Fe bilayer magnetization. A PEEM image confirms that applying a 50-Oe magnetic-field pulse in the opposite direction to the Fe magnetization changes the single-domain state of the Fe film outside the disc to multidomain (Fig. 4b,c). The 50-Oe external magnetic field was turned off during the PEEM measurement so that only the local magnetic field produced by the surrounding Fe film applies to the CoO/Fe disc during the PEEM measurement. Therefore, the local magnetic field produced by the Fe film surrounding the CoO/Fe disc is reduced from $H \sim 32$ Oe in Fig. 4b to $H \sim 0$ in Fig. 4c. Therefore, the position of the Fe vortex core would move back towards the centre of the disc if there were no exchange bias; however, as shown in Fig. 4c, the vortex-core position of the CoO/Fe disc remains virtually unchanged after switching the outside Fe magnetization. This demonstrates that the

exchange-bias effect of the CoO vortex on the Fe vortex is retained even after the magnetic field produced by the surrounding Fe-film magnetization has changed from $H \sim 32$ Oe in Fig. 4b to $H \sim 0$ in Fig. 4c. This is expected because the 32-Oe field is much weaker than the exchange-bias field of the CoO (3 nm)/Fe (12 nm) film so the Fe vortex-core position should remain unchanged after switching off the 32-Oe local magnetic field. To further verify this effect, we warmed the sample back to room temperature. After the sample temperature is raised above the CoO Néel temperature, as demonstrated by the disappearance of the CoO vortex domain (Fig. 4d), we observe that the Fe vortex-core position moves towards the centre of the disc (Fig. 4d), showing the diminishing of the exchange-bias effect of the CoO layer above its Néel temperature.

Our experimental result not only shows the existence of two types of vortex state in the AFM layer of a AFM/FM disc, it also raises many interesting questions for future study. For example, the exchange-bias effect in AFM/FM systems has been mostly studied in continuous films. The exchange-bias field from an AFM vortex state has not been studied deeply, especially the divergent AFM vortex state. To explore the vortex effect on exchange bias, we would need to measure the FM vortex-core position systematically as a function of applied field. Obviously, this kind of study requires different magnetic-domain structures of the surrounding Fe film. Applying an a.c. demagnetization field or a magnetic pulse of different strength could help to realize this. Another new direction could also be developed by imprinting other types of vortex (for example, antivortex and vortex lattice) from the FM layer into the AFM layer.

Methods

NiO/Fe/Ag(001) and CoO/Fe/Ag(001) films were grown epitaxially by molecular beam epitaxy in an ultrahigh-vacuum system with a base pressure of 2×10^{-10} torr. The Fe film was grown by evaporating Fe from a thermal crucible. The NiO and CoO films were grown by evaporating the Ni and Co in an oxygen environment of 10^{-6} torr. The typical evaporation rate is $\sim 1 \text{ \AA min}^{-1}$. Low-energy electron diffraction results show that single-crystalline NiO/Fe and CoO/Fe films were formed with the NiO [110] and CoO [110] axes parallel to the Fe [100] and Ag [110] axes (Fig. 2). The formation of single-crystalline NiO and CoO ensures a non-zero XMLD signal from the NiO and CoO films. After covering the film with a 2-nm-thick Ag protection layer, the films were taken out of the vacuum system and patterned using focused ion-beam patterning (Fig. 2). The sample was measured at both Beamline 4 and the PEEM-3 station of the Advanced Light Source at the

Lawrence Berkeley National Laboratory. In the PEEM-3 station, an electromagnet near the sample holder enables the application of an external magnetic-field pulse to the sample to change the magnetic-domain state of the sample. However, the external magnetic field must be turned off during the PEEM measurement because the Lorentz force exerted on the photoemitted electrons by the external magnetic field prohibits PEEM image acquisition.

For the FM Fe discs, XMCD was used to image the Fe domain at the Fe L3 edge absorption peak. For AFM NiO and CoO discs, XMLD was used to image the NiO and CoO domains at the Ni L2 and Co L3 edge absorption peaks. XMCD measurements on the Ni and Co L edges were also made. The absence of Ni and Co XMCD signal confirms that the XMLD signal is from the antiferromagnetically ordered compensated spins. For the XMLD spectrum measurement (Fig. 1), the Fe magnetization was aligned to its easy magnetization [100] axis, which is parallel to the NiO or CoO [110] axis. Under this condition, the XMLD signal should reach its maximum value when the X-ray polarization axis coincides with the NiO and CoO spin axes. A detailed description can be found in ref. 15.

Received 11 August 2010; accepted 17 November 2010;
published online 23 January 2011

References

- Shinjo, T., Okuno, T., Hassdorf, R., Shigeto, K. & Ono, T. Magnetic vortex core observation in circular dots of permalloy. *Science* **289**, 930–932 (2000).
- Tretiakov, O. A. & Tchernyshyov, O. Vortices in thin ferromagnetic films and the skyrmion number. *Phys. Rev. B* **75**, 012408 (2007).
- Yu, X. Z. *et al.* Real-space observation of a two-dimensional skyrmion crystal. *Nature* **465**, 901–904 (2010).
- Choe, S.-B. *et al.* Vortex core-driven magnetization dynamics. *Science* **304**, 420–422 (2004).
- Van Waeyenberge, B. *et al.* Magnetic vortex core reversal by excitation with short bursts of an alternating field. *Nature* **444**, 461–464 (2006).
- Hertel, R., Gliga, S., Fähnle, M. & Schneider, C. M. Ultrafast nanomagnetic toggle switching of vortex cores. *Phys. Rev. Lett.* **98**, 117201 (2007).
- Yamada, K. *et al.* Electrical switching of the vortex core in a magnetic disk. *Nature Mater.* **6**, 270–273 (2007).
- Vansteenkiste, A. *et al.* X-ray imaging of the dynamic magnetic vortex core deformation. *Nature Phys.* **5**, 332–334 (2009).
- Buchanan, K. S. *et al.* Soliton-pair dynamics in patterned ferromagnetic ellipses. *Nature Phys.* **1**, 172–176 (2005).
- Senthil, T., Vishwanath, A., Balents, L., Sachdev, S. & Fisher, M. P. A. Deconfined quantum critical points. *Science* **303**, 1490–1494 (2004).
- Sort, J. *et al.* Imprinting vortices into antiferromagnets. *Phys. Rev. Lett.* **97**, 067201 (2006).
- Hoffmann, A., Sort, J., Buchanan, K. S. & Nogués, J. Exchange-biased magnetic vortices. *IEEE Trans. Mag.* **44**, 1968–1973 (2008).
- Salazar-Alvarez, G. *et al.* Direct evidence of imprinted vortex states in the antiferromagnet of exchange biased microdisks. *Appl. Phys. Lett.* **95**, 012510 (2009).
- Tanase, M. *et al.* Magnetization reversal in circularly exchange-biased ferromagnetic disks. *Phys. Rev. B* **79**, 014436 (2009).
- Wu, J. *et al.* Direct measurement of rotatable and frozen CoO spins in exchange bias system of CoO/Fe/Ag(001). *Phys. Rev. Lett.* **104**, 217204 (2010).
- Arenholz, E., van der Laan, G., Chopdekar, R. V. & Suzuki, Y. Angle-dependent Ni²⁺ X-ray magnetic linear dichroism: Interfacial coupling revisited. *Phys. Rev. Lett.* **98**, 197201 (2007).
- van der Laan, G., Arenholz, E., Chopdekar, R. V. & Suzuki, Y. Influence of crystal field on anisotropic X-ray magnetic linear dichroism at the Co²⁺L_{2,3} edges. *Phys. Rev. B* **77**, 064407 (2008).
- Nevidomskyy, A. H., Scheiber, C., Sénéchal, D. & Tremblay, A.-M. S. Magnetism and *d*-wave superconductivity on the half-filled square lattice with frustration. *Phys. Rev. B* **77**, 064427 (2008).
- Finazzi, M. *et al.* Interface coupling transition in a thin epitaxial antiferromagnetic film interacting with a ferromagnetic substrate. *Phys. Rev. Lett.* **97**, 097202 (2006).
- Guslienko, K. *et al.* Field evolution of magnetic vortex state in ferromagnetic disks. *Appl. Phys. Lett.* **78**, 3848–3850 (2001).
- Uhlig, T. *et al.* Shifting and pinning of a magnetic vortex core in a permalloy dot by a magnetic field. *Phys. Phys. Lett.* **95**, 237205 (2005).
- Meiklejohn, W. H. & Bean, C. P. New magnetic anisotropy. *Phys. Rev.* **102**, 1413–1414 (1956).
- Nogues, J. & Schuller, I. K. Exchange bias. *J. Magn. Magn. Mater.* **192**, 203–232 (1999).

Acknowledgements

This work was supported by National Science Foundation Grant DMR-0803305, US Department of Energy Grant DE-AC02-05CH11231, the Korea Foundation for International Cooperation of Science and Technology through the Global Research Laboratory project, the Chinese Education Department and the Western Institute of Nanoelectronics.

Author contributions

J.W. and Z.Q.Q. designed and carried out experiments, analysed data and wrote the paper; D.C. and J.B. patterned the discs and wrote the paper; J.S.P., Y.M., E.A., A.D., A.T.Y., A.S., C.H. and H.W.Z. made the X-ray measurements and discussed results.

Additional information

The authors declare no competing financial interests. Reprints and permissions information is available online at <http://npg.nature.com/reprintsandpermissions>. Correspondence and requests for materials should be addressed to Z.Q.Q.